Available online at www.sciencedirect.com
ScienceDirect
Computer Aided Geometric Design 23 (2006) 573–581
COMPUTER AIDED GEOMETRIC DESIGN
www.elsevier.com/locate/cagd

Class A Bézier curves

Gerald Farin

Computer Science and Engineering, PRISM, Arizona State University, Tempe, AZ 85281, USA

Received 2 September 2005; received in revised form 27 March 2006; accepted 30 March 2006

Available online 19 May 2006

Abstract

We discuss 3D Bézier curves with monotone curvature and torsion, generalizing a 2D class of curves by Y. Mineur et al.

1. Introduction

In automotive (and other) design scenarios, many shapes are based on *feature curves* which have to have "perfect" shape in order to produce aesthetically pleasing surfaces. The shape of these curves is primarily defined by their curvature distribution. A "good" curve has a curvature plot (curvature plotted against arc length or parameter) having relatively few regions of monotonically varying curvature (Farin, 2001). Torsion may also play a role as a shape descriptor but seems to be more important in the analysis of robot arm motions. Several articles address curvature of Bézier and B-spline curves: (Beeker, 1986; Sapidis and Farin, 1991; Ferguson et al., 1988; Hoschek, 1984; Roulier, 1988; Meier and Nowacki, 1987; Sánchez-Reyes, 1998; Ueda 1997, 2000a, 2000b). For a book dedicated to the subject, see (Hoschek and Kaklis, 1996).

Ultimately, feature curves will be used to define surfaces, such as car hoods or roofs, or other industrial design surfaces. In the automotive industry, the term "class A surfaces" is used for those parts of a car which are critical for its aesthetic appearance, such as parts of the hood, fender, or roof. The term "class A surface" is reportedly due to the Mercedes-Benz CAD/CAM system SYRKO. Its developers demanded the highest grade of shape quality from the "outside surface" parts, "**A**ussenhaut" in German.[1]

Many of these surfaces are the result of a set of feature curves. For these to qualify to be part of class A surfaces, they have to be "class A" themselves. This paper investigates a family of such curves.

Our work is based on the article (Mineur et al., 1998) (related to work by Ueda (1997)). In it, the authors show that certain 2D Bézier curves—called *typical curves*—are guaranteed to have monotonously increasing or decreasing curvature. The curves are defined by the requirement that each leg of their Bézier polygon is obtained by a rotation and scale of the previous leg, with the rotation and scale being the same for all polygon legs. This translates to

$$\Delta \mathbf{b}_{i+1} = s R \Delta \mathbf{b}_i, \tag{1}$$

E-mail address: gerald.farin@asu.edu (G. Farin).

[1] Literally translated: outside skin.

0167-8396/$ – see front matter
doi:10.1016/j.cagd.2006.03.004

where s is a scale factor, R is a rotation matrix, and where $\Delta\mathbf{b}_i = \mathbf{b}_{i+1} - \mathbf{b}_i$ are the forward difference vectors of the Bézier control points $\mathbf{b}_i$.

Mineur et al. use a notation which limits them to 2D curves. We overcome that restriction by using a different notation.

This work discusses a generalization of the concept of typical curves—however it does not address applications.

2. Class A Bézier curves

A Bézier curve is a 2D or 3D parametric curve whose points $\mathbf{x}(t)$ are defined by

$$\mathbf{x}(t) = \sum_{i=0}^{n} \mathbf{b}_i B_i^n(t).$$

The $\mathbf{b}_i$ are called control points; the B_i^n are Bernstein polynomials; for more details, see (Farin, 2001).

The derivative or hodograph of a Bézier curve is given by

$$\dot{\mathbf{x}}(t) = n \sum_{i=0}^{n-1} \Delta\mathbf{b}_i B_i^{n-1}(t)$$

where $\Delta\mathbf{b}_i = \mathbf{b}_{i+1} - \mathbf{b}_i$.

We will now study a class of special 3D Bézier curves, namely those having hodographs with control vectors

$$\Delta\mathbf{b}_i = \mathbf{v}_i = M^i\mathbf{v}; \quad i = 0, \ldots, n-1, \tag{2}$$

where M is a 3×3 matrix and $\mathbf{v}$ is an arbitrary unit vector.[2] The fact that we stipulate $\mathbf{v}$ to be of unit length is immaterial: Bézier curves are scale invariant, and thus all geometric properties can be studied even if $\mathbf{v}$ is restricted to be of unit length. Under certain conditions on M, curves satisfying (2) will have monotone curvature and torsion. Since such curves are deemed highly desirable in the design of so-called class A surfaces, we will refer to them as *Class A curves.* Fig. 1 gives an example of a cubic Class A curve.

These Class A curves, for any degree n and for a fixed matrix M, form a linear space of dimension two: this is the number of degrees of freedom for a 3D unit vector $\mathbf{v}$. Thus the degrees of freedom in designing with these curves is very low. This makes them ideal candidates for template curves in industrial design environments.

The de Casteljau algorithm (see (Farin, 2001) for details) for the evaluation of a class A hodograph yields a triangular array of the form (shown here for $n = 3$)

$$\begin{array}{lll} \mathbf{v}_0 & & \\ \mathbf{v}_1 & \mathbf{v}_0^1 & \\ \mathbf{v}_2 & \mathbf{v}_1^1 & \mathbf{v}_0^2. \end{array}$$

where

$$\mathbf{v}_i^r(t) = (1-t)\mathbf{v}_i^{r-1}(t) + t\mathbf{v}_{i+1}^{r-1}(t).$$

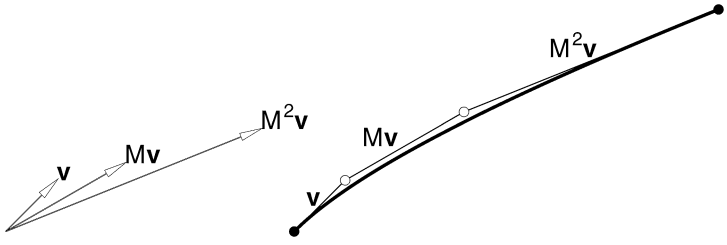

Fig. 1. Class A curves: left, the hodograph vectors; right, the generated curve.

[2] Incidentally, in his work P. Bézier used the difference vectors $\Delta\mathbf{b}_i$ rather than the control points $\mathbf{b}_i$.

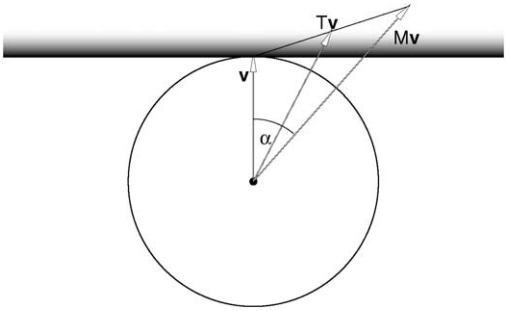

Fig. 2. The vector $M\mathbf{v}$ has to be in the shaded region.

Given the special nature of a Class A hodograph, we have

$$\mathbf{v}_{i+1}^r = M\mathbf{v}_i^r \quad \text{and} \quad \mathbf{v}_{i+1}^r = \mathbf{v}_i^{r-1} + t\big(M\mathbf{v}_i^{r-1} - \mathbf{v}_i^{r-1}\big).$$

We also have

$$\dot{\mathbf{x}}(t) = n\mathbf{v}_0^{n-1} \quad \text{and} \quad \ddot{\mathbf{x}}(t) = n(n-1)\big[\mathbf{v}_1^{n-2} - \mathbf{v}_0^{n-2}\big].$$

We now define Class A curves via the requirement

$$\big\|(1-t)\mathbf{v} + tM\mathbf{v}\big\| \geqslant \big\|\mathbf{v}\big\| \qquad \text{for } t \in [0,1] \text{ and for all } \|\mathbf{v}\| = 1. \tag{3}$$

Geometrically, this means that the line segment $\overline{\mathbf{v}, M\mathbf{v}}$ does not intersect the sphere with radius $\|\mathbf{v}\| = 1$, see Fig. 2. Hence, M may be viewed as an "expansion" matrix. It follows that the angle between $\mathbf{v}$ and $M\mathbf{v}$ must be less than 90 degrees or, equivalently,

$$\cos(\mathbf{v}, M\mathbf{v}) = \frac{\mathbf{v}^{\mathrm{T}} M\mathbf{v}}{\sqrt{\mathbf{v}^{\mathrm{T}} M^{\mathrm{T}} M\mathbf{v}}} \geqslant 0, \tag{4}$$

and this must hold for all unit vectors $\mathbf{v}$.

We square both sides of (3) and obtain

$$(1-t)^2\mathbf{v}^{\mathrm{T}}\mathbf{v} + 2t(1-t)\left[\frac{1}{2}\mathbf{v}^{\mathrm{T}} M\mathbf{v} + \frac{1}{2}\mathbf{v}^{\mathrm{T}} M^{\mathrm{T}}\mathbf{v}\right] + t^2\mathbf{v}^{\mathrm{T}} M^{\mathrm{T}} M\mathbf{v} \geqslant \mathbf{v}^{\mathrm{T}}\mathbf{v}.$$

The expression on the left denotes a quadratic Bézier function with coefficients

$$\mathbf{v}^{\mathrm{T}}\mathbf{v}, \qquad \left[\frac{1}{2}\mathbf{v}^{\mathrm{T}} M\mathbf{v} + \frac{1}{2}\mathbf{v}^{\mathrm{T}} M^{\mathrm{T}}\mathbf{v}\right], \qquad \mathbf{v}^{\mathrm{T}} M^{\mathrm{T}} M\mathbf{v}.$$

If this expression is to exceed $\mathbf{v}^{\mathrm{T}}\mathbf{v}$ for all $t \in [0,1]$, then each coefficient must itself exceed $\mathbf{v}^{\mathrm{T}}\mathbf{v}$, leading to two conditions

$$\mathbf{v}^{\mathrm{T}}\left[\frac{1}{2}M^{\mathrm{T}} + \frac{1}{2}M\right]\mathbf{v} \geqslant \mathbf{v}^{\mathrm{T}}\mathbf{v} \quad \text{and} \quad \mathbf{v}^{\mathrm{T}} M^{\mathrm{T}} M\mathbf{v} \geqslant \mathbf{v}^{\mathrm{T}}\mathbf{v}.$$

Equivalently:

$$\mathbf{v}^{\mathrm{T}}[M^{\mathrm{T}} + M - 2I]\mathbf{v} \geqslant 0 \quad \text{and} \quad \mathbf{v}^{\mathrm{T}}[M^{\mathrm{T}} M - I]\mathbf{v} \geqslant 0. \tag{5}$$

This states that the two symmetric matrices $M^{\mathrm{T}} + M - 2I$ and $M^{\mathrm{T}} M - I$ must be positive definite, and thus must have nonnegative eigenvalues. Note that (5) implies (4).

We now put a further restriction on our matrices, namely that they do not distort too much in the following sense. A sphere is mapped to an ellipsoid by M. The axes of this ellipsoid have lengths $\sigma_1, \sigma_2, \sigma_3$ with $\sigma_1 \geqslant \sigma_2 \geqslant \sigma_3 \geqslant 1$ where the σ_i are the singular values of M, or the square roots of the eigenvalues of $M^{\mathrm{T}} M$. In addition, we also require

$$\sigma_3^2 \geqslant \sigma_1. \tag{6}$$

This additional requirement will be necessary for a proof of curvature and torsion monotonicity in Section 4.

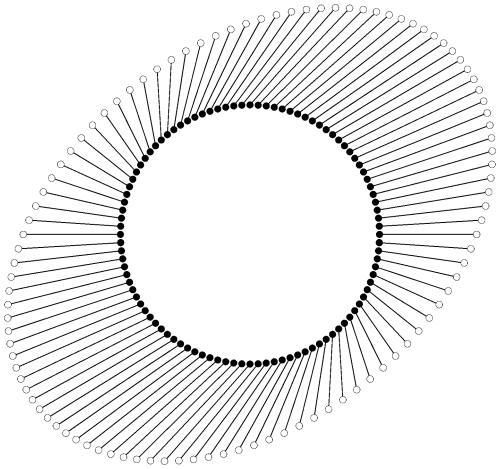

Fig. 3. Action of a Class A matrix.

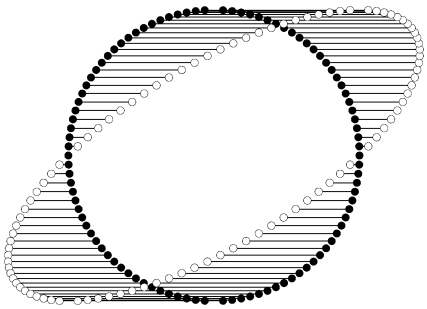

Fig. 4. Action of a non-Class A matrix.

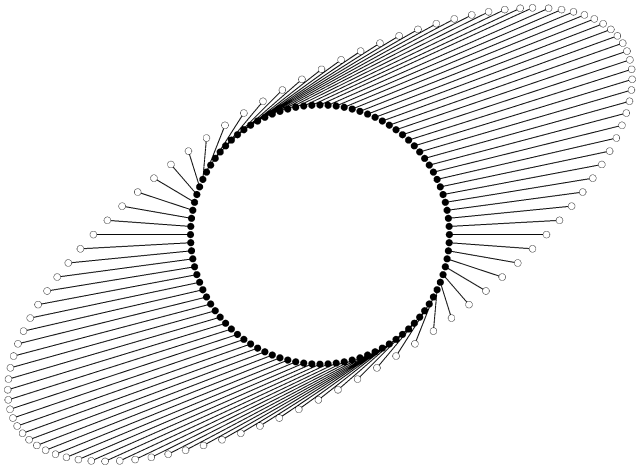

Fig. 5. Action of an "almost" Class A matrix.

A matrix M satisfying both conditions of (5) and also (6), will be called a *Class A matrix*.

Figs. 3, 4, 5 illustrate some geometric aspects of Class A matrices.

Fig. 3 illustrates how a Class A matrix maps a circle to an ellipse. Lines connecting points on the circle and corresponding points on the ellipse never cross the circle. The matrix is a 2D version of the one used later for the third example in Section 5:

$$M = \begin{bmatrix} 1.75 & 0.66 \\ 0 & 1.75 \end{bmatrix}.$$

Fig. 4 also shows a circle and its image, an ellipse. But now some lines connecting points on the circle and corresponding points on the ellipse do cross the circle. The matrix in this case is a shear matrix:

$$M = \begin{bmatrix} 1 & 1 \\ 0 & 1 \end{bmatrix}.$$

Fig. 5 shows the action of a matrix which is "almost" class A. Note that some lines connecting points on the circle and corresponding points on the ellipse (barely) cross the circle. The matrix for this figure is also 2D, and is a modification of the one from the previous figure:

$$M = \begin{bmatrix} 1.75 & 1.66 \\ 0 & 1.75 \end{bmatrix}.$$

Its singular values are 2.8 and 1.1, thus violating (6). However, conditions (5) are met by this matrix.

An example of Class A curves is given by M being composed of a rotation around some axis by an angle $\alpha < 90°$, followed by a scale with factor s. If the condition

$$\cos\alpha > \frac{1}{s} \tag{7}$$

holds, then both conditions (5) are satisfied, and (6) is trivially satisfied. In 2D, the resulting curves are the *typical curves* of (Mineur et al., 1998). In 3D, we refer to them as *3D typical curves*. Fig. 2 illustrates why such curves are Class A.

3. Subdivision

We now show that Class A curves are invariant under subdivision, i.e., if a Class A curve is subdivided, both resulting curves are Class A.

Let us define a linear map T by

$$T\mathbf{v} = (1-t)\mathbf{v} + tM\mathbf{v} = \big[(1-t)I + tM\big]\mathbf{v}$$

with I being the identity matrix.

Then the de Casteljau algorithm scheme takes on the form (here for the case $n = 4$)

$$\begin{array}{cccc} \mathbf{v} & & & \\ M\mathbf{v} & T\mathbf{v} & & \\ M^2\mathbf{v} & MT\mathbf{v} & T^2\mathbf{v} & \\ M^3\mathbf{v} & M^2T\mathbf{v} & MT^2\mathbf{v} & T^3\mathbf{v}, \end{array}$$

i.e., $\mathbf{v}_i^r = M^i T^r \mathbf{v}$.

We quickly verify that $MT = TM$. Hence subdivision generates two segments of the form (2). This is obvious for the diagonal elements $T^i\mathbf{v}$ of the scheme; for the bottom row (which should be traversed from right to left), we observe

$$M^{i+1}T^r = (MT^{-1})M^iT^{r+1},$$

thus the role of M in (2) is now assumed by MT^{-1}.

We still have to verify that both segments are Class A curves, i.e., both T and MT^{-1} satisfy the Class A condition (3). The fact that T satisfies the condition follows from (with $s \in [0,1]$):

$$\begin{aligned} \big\|(1-s)\mathbf{v} + sT\mathbf{v}\big\| &= \big\|(1-s)\mathbf{v} + s(1-t)\mathbf{v} + stM\mathbf{v}\big\| \\ &= \big\|(1-st)\mathbf{v} + stM\mathbf{v}\big\| \\ &\geqslant \|\mathbf{v}\|. \end{aligned}$$

In order to see that MT^{-1} satisfies the Class A condition, we consult Fig. 2 and observe that $MT^{-1}T\mathbf{v} = M\mathbf{v}$, thus showing that MT^{-1} does indeed satisfy the condition.

The above proof will fail if $s \notin [0,1]$: in that case, we would be *extrapolating*. But we cannot make any statements about the behavior of Class A curves outside the domain $[0,1]$. The fact that Class A curves are invariant under subdivision will be used in the next section.

We note that Class A curves are not invariant under another standard operation, namely that of degree elevation: if we apply degree elevation to a Class A control polygon, then the resulting control polygon may violate the Class A conditions.

4. Curvature and torsion

Let us now turn to the curvature of a Class A curve. It is given by

$$\kappa(t) = \frac{\|\dot{\mathbf{x}} \wedge \ddot{\mathbf{x}}\|}{\|\dot{\mathbf{x}}\|^3}.$$

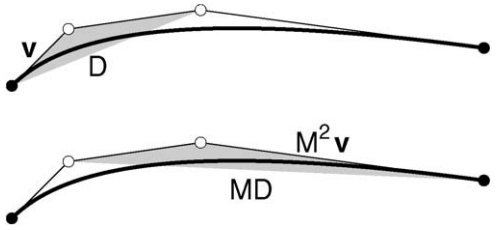

Fig. 6. Monotone curvature: the relevant entities for the cubic case.

We claim that $\kappa(t)$ is monotonically decreasing, i.e., for $\hat{t} \geqslant 0$, we will have $\kappa(\hat{t}) \leqslant \kappa(0)$.

For a proof, let us assume the curve is subdivided at $\hat{t}$ and let us consider only the "left" segment. We know that this segment satisfies the Class A conditions. It is then sufficient to prove that $\kappa(0) \geqslant \kappa(1)$ for this curve segment.

Let $D = [\mathbf{v}, M\mathbf{v}]$ be the (2D) triangle formed by $\mathbf{v}$ and $M\mathbf{v}$, also consult Fig. 6.

We have (see (Farin, 2001)):

$$\kappa(0) = 2\frac{n-1}{n}\frac{|D|}{\|\mathbf{v}\|^3}, \qquad \kappa(1) = 2\frac{n-1}{n}\frac{|M^{n-2}D|}{\|M^{n-1}\mathbf{v}\|^3},$$

with $|D|$ denoting D's area:

$$|D| = \frac{1}{2}\begin{vmatrix} \mathbf{v}^{\mathrm{T}}\mathbf{v} & \mathbf{v}^{\mathrm{T}}M\mathbf{v} \\ \mathbf{v}^{\mathrm{T}}M\mathbf{v} & M^{\mathrm{T}}\mathbf{v}^{\mathrm{T}}M\mathbf{v} \end{vmatrix}^{\frac{1}{2}}.$$

We need to show $\kappa(0) \geqslant \kappa(1)$.

Let us handle the cubic case $n = 3$ first, where we need to show

$$\frac{|D|}{\|\mathbf{v}\|^3} \geqslant \frac{|MD|}{\|M^2\mathbf{v}\|^3}. \tag{8}$$

We denote (in descending order) the singular values of M by $\sigma_1, \sigma_2, \sigma_3$. Then M will "stretch" any vector minimally by σ_3 and maximally by σ_1:

$$\sigma_3\|\mathbf{v}\| \leqslant \|M\mathbf{v}\| \leqslant \sigma_1\|\mathbf{v}\|. \tag{9}$$

Since D and MD share a common edge, the same relationships hold:

$$\sigma_3|D| \leqslant |MD| \leqslant \sigma_1|D|. \tag{10}$$

For a proof of (8), we observe (using (9) and (10)):

$$\frac{|D|}{\|\mathbf{v}\|^3} \geqslant \frac{\frac{1}{\sigma_1}|MD|}{\frac{1}{\sigma_3^3}\|M\mathbf{v}\|^3} = \frac{\sigma_3^3}{\sigma_1}\frac{|MD|}{\|\mathbf{v}\|^3}.$$

Because of the condition (6), we have established (8) since $\|M^2\mathbf{v}\| \geqslant \|M\mathbf{v}\|$.

This argument may be repeatedly applied for degrees exceeding 3.

The analogous argument (utilizing that V and MV share a common face) shows that torsion, given by

$$\tau(t) = \frac{|\dot{\mathbf{x}}, \ddot{\mathbf{x}}, \dddot{\mathbf{x}}|}{\|\dot{\mathbf{x}} \wedge \ddot{\mathbf{x}}\|^2},$$

is monotone for Class A curves since

$$\tau(0) = \frac{3}{2}\frac{n-2}{n}\frac{|V|}{|D|^2}, \qquad \tau(1) = \frac{3}{2}\frac{n-2}{n}\frac{|M^{n-3}V|}{|M^{n-2}D|^2}$$

where

$$V = [\mathbf{v}, M\mathbf{v}, M^2\mathbf{v}]$$

and $|V|$ is V's volume.

5. Examples

We now show some examples. These were chosen to demonstrate that our Class A curves can indeed generate curves as they are needed in real industrial design applications. The curvature and torsion plots are scaled to the same min-max boxes.

Fig. 7 shows the result of using $n = 7$ and

$$\mathbf{v} = \begin{bmatrix} 1 \\ 0 \\ -1 \end{bmatrix}, \qquad M = \begin{bmatrix} 2.52 & 0.53 & 0.34 \\ -0.35 & 2.35 & 0.11 \\ 0 & 0 & 2.58 \end{bmatrix}.$$

The matrix M is a composition of a shear, a scale, and a rotation around the z-axis.

The second example, shown in Fig. 8 is a degree 5 curve, with

$$\mathbf{v} = \begin{bmatrix} -1 \\ 0 \\ 1 \end{bmatrix}, \qquad M = \begin{bmatrix} 2.28 & -0.04 & 0.89 \\ 0.45 & 2.13 & 0.45 \\ 0 & 0 & 2.21 \end{bmatrix}.$$

To the casual observer, it might appear that in the leftmost plot, the curve starts out (from bottom, $t = 0$) with low curvature and then has very high curvature (about $t = 0.2$), thus violating monotonicity. But: that view is jut a projection and does not reveal 3D curve shape!

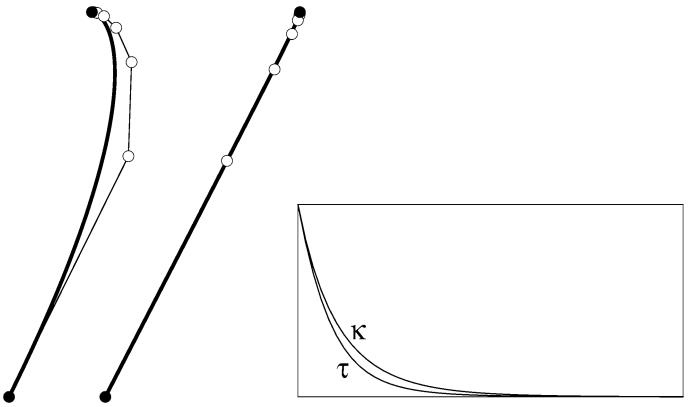

Fig. 7. A degree 7 Class A curve. Left: x, y-view, middle: y, z-view, right: curvature and torsion plots.

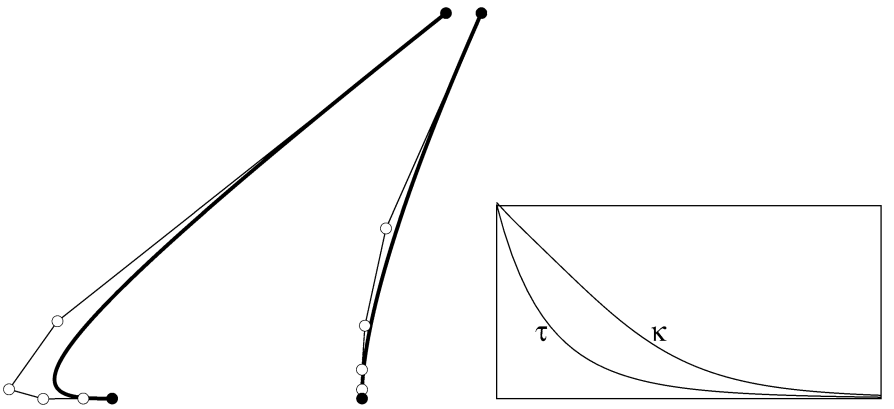

Fig. 8. A degree 5 Class A curve. Left: x, y-view, middle: y, z-view, right: curvature and torsion plots.

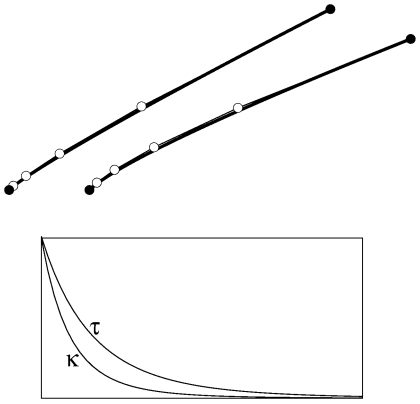

Fig. 9. Another degree 5 Class A curve. Top left: x, y-view, top right: y, z-view, bottom: curvature and torsion plots.

Our final example is shown in Fig. 9; it is again a degree 5 curve, with

$$\mathbf{v} = \begin{bmatrix} 1 \\ 1 \\ 1 \end{bmatrix}, \qquad M = \begin{bmatrix} 1.75 & 0.66 & 0.66 \\ 0 & 1.75 & 0.66 \\ 0 & 0 & 1.75 \end{bmatrix}.$$

The matrix M for this example is upper triangular; it has no rotational component.

6. An application

Suppose we are given two beginning and ending 3D tangent vectors, $\mathbf{v}_0$ and $\mathbf{v}_n$, respectively.[3] We are asking if there are degree *n 3D typical curves* having these as beginning and ending tangent vectors. In other words, is there a rotation matrix R and a stretch factor $s > 1$ such that the sequence of vectors $s^i R^i \mathbf{v}_0$ describes the hodograph of a 3D typical curve? Clearly R must be a rotation by Γ/n around the axis $\mathbf{v}_0 \wedge \mathbf{v}_n$, where Γ is the angle formed by $\mathbf{v}_0$ and $\mathbf{v}_n$. Similarly, $s = (\|\mathbf{v}_n\|/\|\mathbf{v}_0\|)^{1/n}$. The condition (7) becomes

$$\cos(\Gamma/n) > \frac{1}{s}. \tag{11}$$

For an arbitrarily given n, this condition may not be satisfied. But if we increase n sufficiently, it will be met eventually. If we treat n as a real number n', we may ask when equality holds in (11), thus obtaining

$$\cos(\Gamma/n') = \frac{1}{s}.$$

Thus

$$n' = \Gamma/\operatorname{acos} \frac{1}{s}$$

and hence any $n \geqslant n'$ will give rise to a 3D typical curve. Note that the degree n will be the higher the closer s is to 1.

7. Conclusion and future work

We presented a class of curves which are a generalization of the typical curves by Mineur et al.

We only discussed monotonicity for curvature and torsion. In practice, convexity of these functions is also an important consideration. More work is needed to address this problem.

This research is mostly theoretical in that it does not give constructive algorithms for general Class A curves. Theoretically, a Class A Bézier curve is defined by its degree, a vector $\mathbf{v}$ and a matrix M. In practice, a designer

[3] We assume $\|\mathbf{v}_n\| > \|\mathbf{v}_0\|$.

might want to fit a Class A curve to digitized points. Mineur et al. presented algorithms to do this for 2D typical curves—similar methods need to be developed for our Class A curves.

We do not offer a method for finding a matrix M and a vector $\mathbf{v}$ in order to achieve a design objective. However, it must be noted that there is an interplay between M and $\mathbf{v}$. If M has real eigenvalues and $\mathbf{v}$ is a corresponding eigenvector, then the resulting curve will be a straight line. Hence, it appears that the proximity of $\mathbf{v}$ to M's eigenvectors is closely related to the shape of the resulting curve.

Next, while Bézier curves are important, the truly ubiquitous curve tool are B-spline curves. Our results will need to be generalized to these curves.

Surfaces are much more important than curves in a design environment. The topic of Class A surfaces is addressed by (Anderson et al. 1987, 1988; Andersson, 1993; Farin, 1983; Hagen, 1986; Wang et al., 2003; Loh, 1981; Kaklis and Ginnis, 1996). We are working on a generalization of Class A curves to surfaces as follows:

$$\mathbf{b}_{i+1,j} - \mathbf{b}_{i,j} = U^i \mathbf{u}, \qquad \mathbf{b}_{i,j+1} - \mathbf{b}_{i,j} = V^j \mathbf{v}, \tag{12}$$

meaning that all u- and v-control grid lines are polygons of Class A curves defined by Class A matrices U and V. We will report on this elsewhere.

References

Andersson, E., Andersson, R., Boman, M., Dahlberg, B., Elmroth, T., Johansson, B., 1988. Automatic construction of surfaces with prescribed shape. Computer Aided Design 20 (6), 317–324.

Andersson, R., 1993. Surfaces with prescribed curvature I. Computer Aided Geometric Design 10 (5), 431–452.

Andersson, R., Andersson, E., Boman, M., Dahlberg, B., Elmroth, T., Johansson, B., 1987. The automatic generation of convex surfaces. In: Martin, R. (Ed.), The Mathematics of Surfaces II. Oxford University Press, pp. 427–446.

Beeker, E., 1986. Smoothing of shapes designed with free-form surfaces. Computer Aided Design 18 (4), 224–232.

Farin, G., 1983. Some aspects of car body design at Daimler-Benz. In: Barnhill, R., Boehm, W. (Eds.), Surfaces in Computer Aided Geometric Design. North-Holland, pp. 93–98.

Farin, G., 2001. Curves and Surfaces for Computer Aided Geometric Design, fifth ed. Morgan Kaufmann.

Ferguson, D., Frank, P., Jones, A., 1988. Surface shape control using constrained optimization on the B-spline representation. Computer Aided Geometric Design 5 (2), 87–103.

Hagen, H., 1986. Bézier-curves with curvature and torsion continuity. The Rocky Mountain Journal of Mathematics 16 (3), 629–638.

Hoschek, J., 1984. Detecting regions with undesirable curvature. Computer Aided Geometric Design 1 (2), 183–192.

Hoschek, J., Kaklis, P. (Eds.), 1996. FAIRSHAPE. Teubner, Stuttgart.

Kaklis, P., Ginnis, A., 1996. Sectional-curvature preserving skinning surfaces. Computer Aided Geometric Design 13 (7), 601–619.

Loh, R., 1981. Convex B-spline surfaces. Computer Aided Design 13 (3), 145–149.

Meier, H., Nowacki, H., 1987. Interpolating curves with gradual changes in curvature. Computer Aided Geometric Design 4 (4), 297–305.

Mineur, Y., Lichah, T., Castelain, J.M., Giaume, H., 1998. A shape controlled fitting method for Bézier curves. Computer Aided Geometric Design 15 (9), 879–891.

Roulier, J., 1988. Bézier curves of positive curvature. Computer Aided Geometric Design 5 (1), 59–70.

Sánchez-Reyes, J., 1998. Harmonic rational Bézier curves, p-Bézier curves and trigonometric polynomials. Computer Aided Geometric Design 15 (9), 909–923.

Sapidis, N., Farin, G., 1991. Shape preservation and the fairness of curves. Computer Aided Design 23 (6), 460. Letter to the Editor.

Ueda, K., 1997. A sequence of Bézier curves generated by successive pedal-point constructions. In: Le Méhauté, A., Rabut, C., Schumaker, L. (Eds.), Curves and Surfaces with Applications in CAGD. Vanderbilt University Press, pp. 427–434.

Ueda, K., 2000a. Pedal curves and surfaces. In: Lyche, T., Schumaker, L. (Eds.), Mathematical Methods for Curves and Surfaces. Vanderbilt University Press, pp. 497–507.

Ueda, K., 2000b. Polar curves and surfaces. In: Cipolla, R., Martin, R. (Eds.), The Mathematics of Surfaces IX. Springer-Verlag, pp. 372–388.

Wang, Y., Wang, S., Zhang, L., Zhao, B., 2003. Shape control of Bézier surfaces with iso-parametric monotone curvature constraints. Computer Aided Geometric Design 20 (6), 383–394.